

SMART

Unbalance response and stability analyses of the rotor of SMART Main Coolant Pump

150

SMART (MCP) 가 . 가 MCP

Abstract

SMART main coolant pump(MCP) is being designed as a vertical type and the rotor is operated immersed in hot and high pressure water. Hydraulic forces which are taken place at journal bearings, impellers and gaps between rotor and housing are inherently highly nonlinear and have unstable characteristics. Furthermore, since vertical rotor rather than horizontal type has no dominant static bearing load such as one's weight, traveling of journal center in the clearance circle of the bearing as varying of rotational speed make change in rotor characteristics greatly. In this paper, MCP rotor dynamic characteristics are estimated relating in hydraulic forces at journal bearings and gaps.

1.

(MCP) SMART , 10
 가 . MCP
 가 . MCP
 가 . MCP

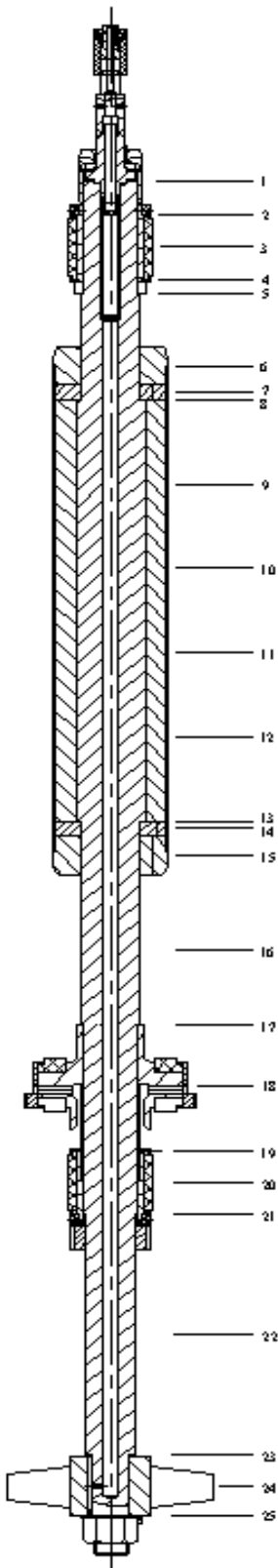


Fig. 1 MCP rotor model

Fig 1
Timoshenko
Table 2

3

Fig. 2 MCP

2.

MCP

37.581kg,
65.300kg

12

MCP

MCP

가

Table 1

24

[1].

가

Table

1/2

27.639kg
1.378m

4

4

$$-\begin{Bmatrix} F_x \\ F_y \end{Bmatrix} = \begin{bmatrix} K_{xx} & K_{xy} \\ K_{yx} & K_{yy} \end{bmatrix} \begin{Bmatrix} X \\ Y \end{Bmatrix} + \begin{bmatrix} C_{xx} & C_{xy} \\ C_{yx} & C_{yy} \end{bmatrix} \begin{Bmatrix} \dot{X} \\ \dot{Y} \end{Bmatrix}$$

12

가

[2].

$$\frac{1}{R^2} \frac{\partial}{\partial \theta} \left(G_\theta \frac{h^3}{\mu} \frac{\partial p}{\partial \theta} \right) + \frac{\partial}{\partial z} \left(G_z \frac{h^3}{\mu} \frac{\partial p}{\partial z} \right) = \frac{1}{2} \omega \frac{\partial h}{\partial \theta} + \frac{\partial h}{\partial t}$$

[3].

$$G_\theta = \frac{l}{12 + 0.0136R_e^{0.9}}, G_z = \frac{l}{12 + 0.0043R_e^{0.96}}$$

$$R_e (= \frac{\rho U h}{\mu})$$

(Couette Reynolds number), $U (= \omega R)$

$$, G_\theta = G_z = \frac{l}{12}$$

Fig. 3

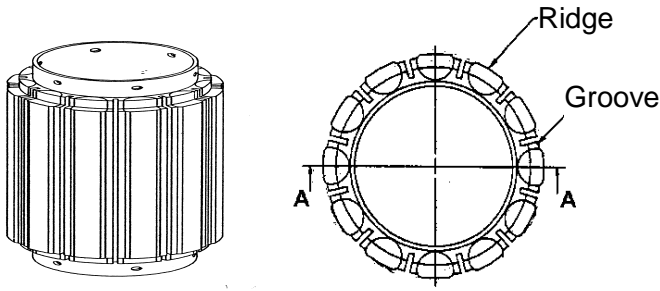


Fig. 2 Configuration of MCP journal bearing properties

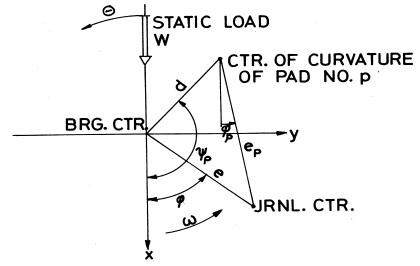


Fig. 3 Coordinate of bearing to calculate properties

[4].

$$\left\{ \frac{1}{R^2} \frac{\partial}{\partial \theta} \left(G_\theta \frac{h_0^3}{\mu} \frac{\partial}{\partial \theta} \right) + \frac{\partial}{\partial z} \left(G_z \frac{h_0^3}{\mu} \frac{\partial}{\partial z} \right) \right\} \begin{Bmatrix} p_0 \\ p_x \\ p_y \\ p_{\dot{x}} \\ p_{\dot{y}} \end{Bmatrix} = \begin{Bmatrix} \frac{1}{2} \omega \frac{\partial h_0}{\partial \theta} \\ -\frac{1}{2} \omega \left(\sin \theta + 3 \frac{\cos \theta}{h_0} \frac{\partial h_0}{\partial \theta} \right) - 3G_\theta \frac{h_0^3}{R^2 \mu} \frac{\partial p_0}{\partial \theta} \frac{\partial}{\partial \theta} \left(\frac{\cos \theta}{h_0} \right) \\ \frac{1}{2} \omega \left(\cos \theta - 3 \frac{\sin \theta}{h_0} \frac{\partial h_0}{\partial \theta} \right) - 3G_\theta \frac{h_0^3}{R^2 \mu} \frac{\partial p_0}{\partial \theta} \frac{\partial}{\partial \theta} \left(\frac{\sin \theta}{h_0} \right) \\ \cos \theta \\ \sin \theta \end{Bmatrix}$$

($\frac{\partial p}{\partial z} = 0$)

[5].

$$\frac{1}{R^2} \frac{\partial}{\partial \theta} \left(G_\theta \frac{h_0^3}{\mu} \frac{\partial}{\partial \theta} \right) \begin{Bmatrix} p_0 \\ p_x \\ p_y \\ p_{\dot{x}} \\ p_{\dot{y}} \end{Bmatrix} = \begin{Bmatrix} \frac{1}{2} \omega \frac{\partial h_0}{\partial \theta} \\ -\frac{1}{2} \omega \left(\sin \theta + 3 \frac{\cos \theta}{h_0} \frac{\partial h_0}{\partial \theta} \right) - 3G_\theta \frac{h_0^3}{R^2 \mu} \frac{\partial p_0}{\partial \theta} \frac{\partial}{\partial \theta} \left(\frac{\cos \theta}{h_0} \right) \\ \frac{1}{2} \omega \left(\cos \theta - 3 \frac{\sin \theta}{h_0} \frac{\partial h_0}{\partial \theta} \right) - 3G_\theta \frac{h_0^3}{R^2 \mu} \frac{\partial p_0}{\partial \theta} \frac{\partial}{\partial \theta} \left(\frac{\sin \theta}{h_0} \right) \\ \cos \theta \\ \sin \theta \end{Bmatrix}$$

Table 1

34 , L/2 7

Table 1 Bearing fluidal and geometrical data

Properties	No of pad	Radius mm	Length mm	Pad radial clearance, μm	Ambient pressure Mpa	Temperatur e $^{\circ} c$	Absolute viscosity of water, N-s/m ²	Density, kg/m ³
UBR	12	45	58	65	14.7	70	0.00041	984
LBR	12	45	58	65	14.7	150	0.000186	925

가

$$-\begin{Bmatrix} F_x \\ F_y \end{Bmatrix} = \begin{bmatrix} K_{xx} & K_{xy} \\ K_{yx} & K_{yy} \end{bmatrix} \begin{Bmatrix} X \\ Y \end{Bmatrix} + \begin{bmatrix} C_{xx} & C_{xy} \\ C_{yx} & C_{yy} \end{bmatrix} \begin{Bmatrix} \dot{X} \\ \dot{Y} \end{Bmatrix} + \begin{bmatrix} M_{xx} & M_{xy} \\ M_{yx} & M_{yy} \end{bmatrix} \begin{Bmatrix} \ddot{X} \\ \ddot{Y} \end{Bmatrix}$$

가

(

(concentric annular seal)

Black

[2,5].

$$-\frac{\lambda}{\pi R P} \begin{Bmatrix} F_x \\ F_y \end{Bmatrix} = \begin{bmatrix} \mu_0 - \frac{1}{4} \mu_2 \omega^2 T^2 & \frac{1}{2} \mu_1 \omega T \\ -\frac{1}{2} \mu_1 \omega T & \mu_0 - \frac{1}{4} \mu_2 \omega^2 T^2 \end{bmatrix} \begin{Bmatrix} X \\ Y \end{Bmatrix} + \begin{bmatrix} \mu_1 T & \mu_2 \omega T^2 \\ -\mu_2 \omega T^2 & \mu_1 T \end{bmatrix} \begin{Bmatrix} \dot{X} \\ \dot{Y} \end{Bmatrix} + \begin{bmatrix} \mu_2 T^2 & 0 \\ 0 & \mu_2 T^2 \end{bmatrix} \begin{Bmatrix} \ddot{X} \\ \ddot{Y} \end{Bmatrix}$$

.λ

$$\lambda = 0.079 R_a^{-1/4} \{1 + (7/8 R_r / R_a)^2\}^{3/8}$$

, $R_a (= 2\rho C_r V_s / \mu)$:

, $R_r (= \rho \omega R C_r / \mu)$:

, ρ :

, μ :

, C_r :

, $T (= L/V_s)$:

가

, L :

, $V_s (= Q/(2.0\pi R C_r))$:

, Q :

, ω :

, R :

P Yamaha

$$P = (1 + \xi + 2\sigma) \frac{\rho V_s^2}{2}$$

$\sigma (= \lambda(L/C_r))$:

, ξ

0.2845

0.5

μ₀, μ₁, μ₂

$$\mu_0 = \frac{(1 + \xi)\sigma^2}{(1 + \xi + 2\sigma)^2}$$

$$\mu_1 = \frac{(1 + \xi)^2 \sigma + (1 + \xi)(2.33 + 2\xi)\sigma^2 + 3.33(1 + \xi)\sigma^3 + 1.33\sigma^4}{(1 + \xi + 2\sigma)^3}$$

$$\mu_2 = \frac{0.33(1 + \xi)^2 (2\xi - 1)\sigma + (1 + \xi)(1 + 2\xi)\sigma^2 + 2(1 + \xi)\sigma^3 + 1.33\sigma^4}{(1 + \xi + 2\sigma)^4}$$

가

(L/D << 1)

[7].

$$\mu_0\left(\frac{L}{R}\right) = \frac{\mu_0}{1+0.28(L/R)^2}, \mu_1\left(\frac{L}{R}\right) = \frac{\mu_1}{1+0.23(L/R)^2}, \mu_2\left(\frac{L}{R}\right) = \frac{\mu_2}{1+0.06(L/R)^2}$$

Black

[8].

$$-\begin{Bmatrix} F_x \\ F_y \end{Bmatrix} = \begin{bmatrix} -\frac{1}{4}m_a\omega^2 & k\omega \\ -k\omega & -\frac{1}{4}m_a\omega^2 \end{bmatrix} \begin{Bmatrix} X \\ Y \end{Bmatrix} + \begin{bmatrix} 2k & m_a\omega \\ -m_a\omega & 2k \end{bmatrix} \begin{Bmatrix} \dot{X} \\ \dot{Y} \end{Bmatrix} + \begin{bmatrix} m_a & 0 \\ 0 & m_a \end{bmatrix} \begin{Bmatrix} \ddot{X} \\ \ddot{Y} \end{Bmatrix}$$

$$m_a (= \rho R^3 L / C_r)$$

, μ_e

$$k (= 0.0053 \mu R_r^{0.75})$$

. Table 2

$$k (= 6 \mu_e L (R/C_r)^3)$$

Table 2 Fluid and geometrical data of the gap

Properties	Radius mm	Length Mm	Radial clearance, mm	Temperature °c	Axial flow rate, m ³ /s	Absolute viscosity of water, N-s/m ²	water density, kg/m ³
Motor gap	53	519	1.4	70	8.333x10 ⁻⁴	0.00041	984
Impeller gap	23	223	0.8	200	4.1667x10 ⁻⁶	0.000137	874

Table 3

10⁴ N/m
가 3600RPM

MCP

3

. Fig. 4

3

. 2

1

가

. 3

가

가

1

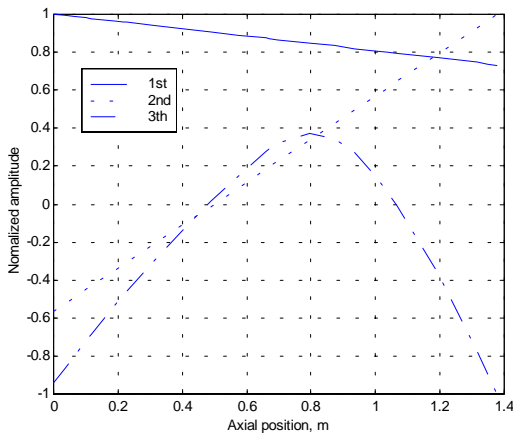


Fig. 4 First three mode shapes of the MCP

Table 3 Variations of the natural frequencies by changing inner hole diameter in the MCP rotor

mode freq. (RPM)	3B	3F	4B	4F	5B	5F
	6162.3	6322.3	16331.1	16616.3	30225.5	30761.8

MCP
가

$$F_r = K_r \gamma HDB$$

F_r : , K_r : MCP 가 , γ : 가 , H , D : , B :
가
[12] 0.05 2Newton
(0.9665m), (0.346m)
0.8, 2.9Newton 180 °
2, 6Newton . Table 4, 5 3600RPM
. Fig 5 . MCP
가

Table 4 Dynamic properties of gap at 3600 RPM

Properties	Stiffness, N/m		Damping, N/m-s		Mass, Kg
	Kyy, Kzz	Kyz, -Kzy	Cyy, Czz	Cyz, -Czy	
Motor gap	-2.7 x10 ⁵	3.3 x10 ⁵	1732.7	28802	76.4
Impeller gap	-3.5 x10 ⁵	87051	461.8	3715.5	9.9

Table 5 Dynamic properties of plain journal bearing at 3600 RPM

Properties	Radial Reynolds No.	Stiffness, N/m				Damping, N-s/m			
		Kyy	Kyz	Kzy	Kzz	Cyy	Cyz	Czy	Czz
UBR	2504	0.2	6.0 x10 ⁵	-5.9 x10 ⁵	-1.0	3009.6	0	0	3029
LBR	5062	2.9	4.7 x10 ⁵	-4.1 x10 ⁵	-3.4	2149.3	0.2	0	2371.6

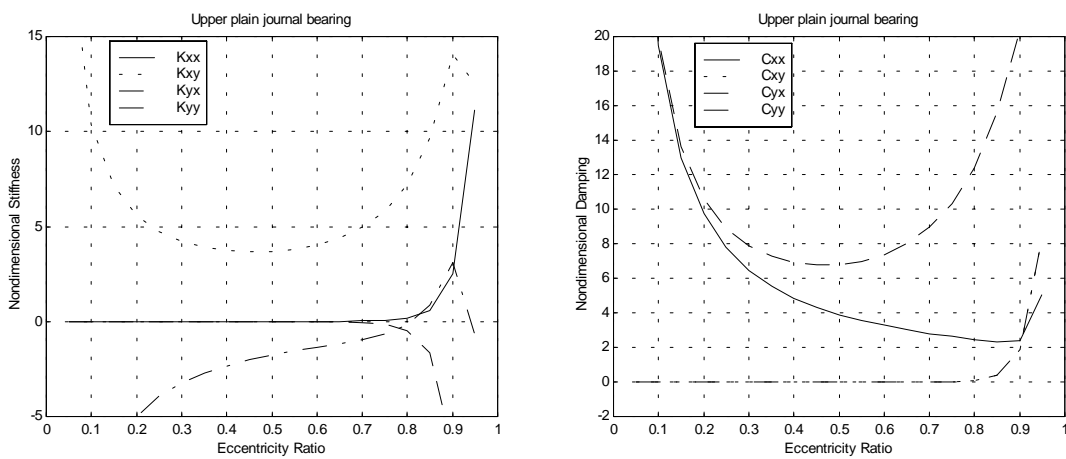


Fig. 5 Stiffness and damping properties of MCP journal bearing with eccentricity ratio at 3600RPM

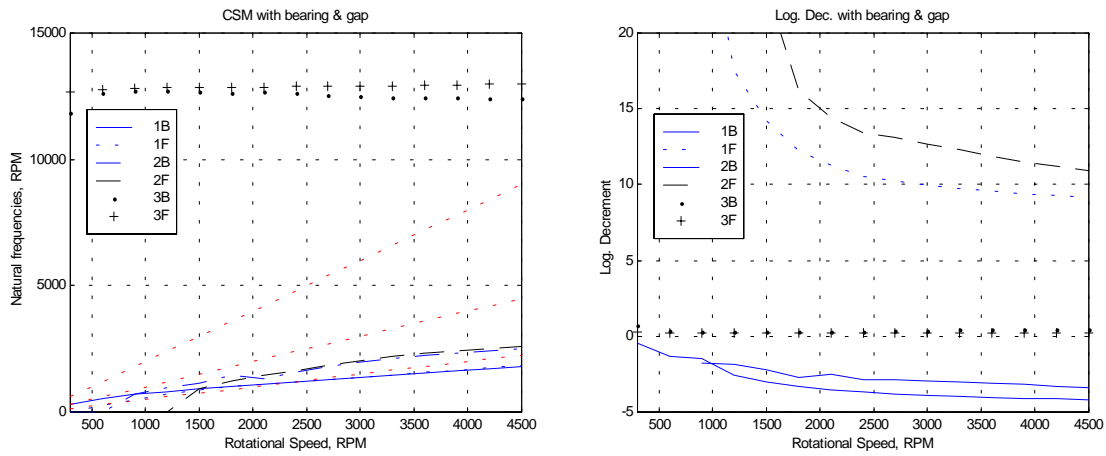


Fig. 6 Natural frequencies and log. decrements of MCP rotor with varying rotational speed

가

MCP

$$s_i = \sigma_i + j\omega_i$$

가

$$\delta_i = \frac{2\pi\sigma_i}{\omega_i}$$

Fig 6

300 ~ 4500 RPM

(damped natural frequency)

(logarithmic decrement)

0.5X, 1X, 2X

가

. 2000RPM

1

가

. 1B, 2B

가

가

가

. 3600RPM

-15% ~+20%

가

가

10kg

50 μ m

500g-mm

가

3600RPM

$$mr\Omega^2 = 10 \times 50 \times 10^{-6} \times (60 \times 2 \times \pi)^2 = 71 \text{ Newton.}$$

Fig. 7

가

2200RPM

가 가

. 1000RPM

3600pm

API

3800 RPM

2.5G

2.9G

$$G = \frac{\epsilon \omega}{1000}$$

: (g-mm) / (kg), : (rad/s)

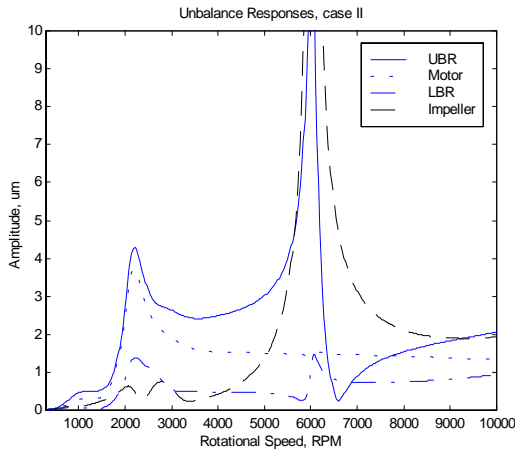


Fig. 7 Unbalance responses of the MCP rotor with bearing and gap dynamics

3.

MCP

가

MCP

1

3

가

가

가

MCP

가

가

MCP

(quasi-linear)

가가

1 Hashish, E. and Sanker, T. S., "Finite element and modal analyses of rotor bearing systems under stochastic loading conditions," Trans. ASME, Journal of Vibration, Acoustics, Stress and Reliability in Design, 1984, Vol.106, pp.80-89

2 T. Someya. Journal-Bearing Databook. Springer-Verlag, NewYork, 1989

3 V.N. Constantinescu, Basic Relationships in Turbulent Lubrication and Their Extension to Include Thermal Effects. ASME Journal of Lubrication Tech., 1973, 95 (2):pp147-154

4 J.W. Lund, K.K.Thomsen, A calculation method and data for the dynamic coefficients of oil-lubricated journal bearings', Conf. Of design engineering 1978 pp1-28

5 , 1998

6 Rainer Nordmann, Harald Massman, 'Identification of dynamic coefficients of annular turbulent seals', Proceedings of workshop for rotordynamic instability, Texas A & M University, 1984, pp.295-311

7 Chan Siu Hung, 'Nonlinear analysis of rotordynamic instabilities in high-speed turbomachinery', Ph.D dissertation, Trondheim Univ. (Norway), 1992

8 H.F. Black, Effects of Fluid-filled clearance Spaces on centrifugal pump and submerged motor vibrations, Proceedings of 8th turbomachinery symposium, Texas A & M University, pp.29-38, 1979